In vivo validation of a new portable stimulator for chronic deep brain stimulation in freely moving rats

Houyam Tibar, Frédéric Naudet, Florian Kolbl, Bastien Ribot, Emilie Faggiani, Gilles N'kaoua, Sylvie Renaud, Noëlle Lewis, Abdelhamid Benazzouz

Version of Record: https://www.sciencedirect.com/science/article/pii/S0165027019304340
Manuscript_4934e7f74603ccaf3d57a78fa3d48599

In vivo validation of a new portable stimulator for chronic deep brain stimulation in freely moving rats

Houyam Tibar[1,2,*], Frédéric Naudet,[1,2,*] Florian Kölbl[3,*], Bastien Ribot,[1,2] Emilie Faggiani,[1,2] Gilles N'Kaoua,[3] Sylvie Renaud,[3] Noëlle Lewis[3], and Abdelhamid Benazzouz[1,2,$]

* These authors contributed equally

1. Univ. de Bordeaux, Institut des Maladies Neurodégénératives, UMR 5293, F-33000 Bordeaux, France.

2. CNRS, Institut des Maladies Neurodégénératives, UMR 5293, F-33000 Bordeaux, France.

3. Univ. de Bordeaux, Department of Bioelectronic, Laboratory IMS-CNRS UMR 5218, F-33000 Bordeaux, France.

[$] Correspondances should be addressed to Dr. Abdelhamid Benazzouz, Institut des Maladies Neurodégénératives (IMN), CNRS UMR 5293, Centre Broca Nouvelle-Aquitaine, Université de Bordeaux, 146, Rue Léo-Saignat, 33076 Bordeaux Cedex, France.
E-mail: Abdelhamid.Benazzouz@u-bordeaux.fr
Tel: +33 5 33 51 48 03; Fax: +33 556 90 14 21

Declaration of interest: none

Abstract

Background. Deep brain stimulation (DBS) of the subthalamic nucleus (STN) is considered as a gold standard therapy for the alleviation of motor symptoms in Parkinson's disease (PD). This success paved the way to its application for other neurological and psychiatric disorders. In this context, we aimed to develop a rodent-specific stimulator with characteristics similar to those used in patients.

New method. We designed a stimulator that can be connected to an electrode container with options for bilateral or unilateral stimulation selection and offers a wide range of frequencies, pulse widths and intensities, constant current, biphasic current-control and charge balancing. Dedicated software was developed to program these parameters and the device was tested on a bilateral 6-hydroxydopamine (6-OHDA) rat model of PD.

Results. The equipment was well tolerated by the animals with a good general welfare. STN stimulation (130 Hz frequency, 0.06 ms pulse width, 150 µA average intensity) improved the motor deficits induced by 6-OHDA as it significantly increased the number of movements compared to the values obtained in the same animals without STN stimulation. Furthermore, it restored motor coordination by significantly increasing the time spent on the rotarod bar.

Conclusion. We successfully developed and validated a new portable and programmable stimulator for freely moving rats that delivers a large range of stimulation parameters using bilateral biphasic current-control and charge balancing to maximize tissue safety. This device can be used to test deep brain stimulation in different animal models of human brain diseases.

Key words: Deep brain stimulation; High frequency stimulation; Chronic stimulation; Portable stimulator; Parkinson's disease; Animal models.

Highlights

- We successfully developed a new portable stimulator for freely moving rats.
- The device is characterized by the large range of stimulation parameters.
- The device delivers biphasic current-control and charge balancing to maximize tissue safety.
- Bilateral stimulation improved severe motor deficits in the 6-OHDA rat model of Parkinson's disease.
- The device can be used to test deep brain stimulation in different animal models of human brain diseases.

1. Introduction

High frequency stimulation (HFS) of deep brain structures, named deep brain stimulation (DBS), is now a recognized therapeutic approach used for the treatment of a wide range of neurological and psychiatric disorders (Krack et al., TINS 2010). Parkinson's disease (PD) is the first neurological condition to benefit from DBS when dopaminergic treatments are no longer tolerated by patients (Lang and Lozano, 1998). Animal studies have been developed in rodents and non-human primates to better understand the pathophysiology of PD and to develop new therapeutic approaches. Indeed, HFS of the subthalamic nucleus (STN) alleviated the cardinal motor symptoms induced by the neurotoxin 1-methyl-4-phenyl-1,2,3,6-tetrahydropyridine (MPTP) in a non-human primate model of the disease (Benazzouz et al., 1993). Then, STN-HFS was transferred and successfully applied to parkinsonian patients with advanced severe motor symptoms (Limousin et al., 1995). The electrodes are implanted chronically and connected to an implantable stimulator delivering continuous HFS to improve the symptoms.

STN-HFS is now considered as an alternative treatment of choice proposed to parkinsonian patients when they develop motor fluctuations and dyskinetic involuntary abnormal movements in response to medication (Limousin et al., 1995; 1998; Krack et al., 2003). However, although the beneficial effects of STN-HFS are well established, the underlying mechanisms are still under debate (Benazzouz and Halett, 2000; Tai et al., 2003; Meissner et al., 2005; Salin et al., 2002; Faggiani and Benazzouz, 2017; Schor and Nelson, 2019). Understanding the functional mechanisms should lead to the improvement of DBS therapy and devices, as well as characterizing and minimizing the potential related side effects. While several side effects are linked to surgery, others, such as mood and cognitive changes, dysarthria, verbal fluency decrease, exacerbation of gait disorders, and weight gain have also been reported and may be related to the spread of current to the surrounding areas

of the STN (Temel et al., 2005; Krack et al., 2010). In this regard, there is a need for further investigations in animal models of PD. Moreover, the success of DBS in PD, and its reversibility in contrast to ablation of brain structures, paved the way to its application in other neurological and psychiatric disorders.

The present study aimed to develop a new DBS dedicated stimulator adapted for chronic experiments on rodents and that mimics the conditions of DBS human therapy. In addition to this objective, the device was developed to be highly configurable and tunable to allow for various investigations. Dedicated software was also developed to program the stimulation parameters and the device was tested on a bilateral 6-hydroxydopamine (6-OHDA) rat model of PD.

2. Materials and Methods

2.1. Animals and ethics statement

Adult male Sprague-Dawley rats weighing 280-300g at the start of the experiments were used. They were housed four per cage in a temperature and humidity-controlled room with a 12-hour light/dark cycle with food and water available *ad libitum*. Surgical and experimental procedures were performed in accordance with the European Community's Council Directive (*EU Directive 2010/63/EU*86) and the National Institute of Health Guide for the Care and Use of laboratory animals. The protocol was approved by the Ethics Committee for Animal Experiments of Bordeaux (Comité d'éthique de Bordeaux en expérimentation animale; Permit Number 50120135-A). All efforts were made to minimize animal suffering. The experimental paradigm is summarized in Figure 1.

2.2. Dopamine depletion procedures

A total of 24 rats were used in this study and subdivided into two groups, 6-OHDA-lesioned rats (n=14) and sham-operated rats (n=10). They received stereotactic bilateral microinjections of either 6-hydroxydopamine (6-OHDA, Sigma, Saint-Quentin Fallavier, France) or saline (NaCl 0.9%) into the medial forebrain bundle (MFB) as previously described (Faggiani et al., 2018). After administration of xylazine (xylazine hydrochloride, 10 mg/kg, i.p., Sigma) and ketamine anaesthesia (ketamine hydrochloride, 75 mg/kg, i.p. Sigma), rats were placed in a stereotaxic frame (Kopf, Unimecanique, France). Thirty minutes before the stereotaxic injection of 6-OHDA, animals received an i.p. injection of desipramine (25 mg/kg, i.p., Sigma) to protect noradrenergic neurons. Desipramine was dissolved in 0.9% NaCl and injected in a volume of 5 ml/kg body weight. Each animal received a bilateral injection of 2.5 µl 6-OHDA (1.67 mg/ml in sterile NaCl, 0.9%) with 0.1% ascorbic acid into both MFB over a 5 minute period using a 10 µl Hamilton microsyringe. The coordinates were 2.8 mm posterior to bregma (AP), 2 mm lateral to the midline (L) and 8.4 mm below the skull (D), according to the brain atlas of Paxinos and Watson (1996). After surgery, the rats were returned to the animal facility with food and water available *ad libitum*. To avoid the loss of animals common with the bilateral injection of 6-OHDA, they were nursed and fed with additional cereals, apple and formula milk for five days.

2.3. Implantation of the stimulating electrodes and the portable stimulator

Three weeks after the bilateral injection of 6-OHDA or saline into the MFB, the stimulating electrodes were implanted bilaterally into the STNs of animals of the two groups under ketamine and xylazine anaesthesia, as previously described (Faggiani et al., 2015). Rats were placed in a stereotaxic frame and holes were drilled over the right and left STNs (Figure 2, AP: -3.8, ML: 2.5), according to the rat brain atlas (Paxinos & Watson, 1996). Six screws were placed and fixed on the skull and covered with dental cement (Dentalon Plus, Heraeus

Kulzer, USA). We designed an electrode container consisting of a mechanical plastic plate in which two bipolar platinum/iridium electrodes were inserted. The two electrodes were built with a 5 mm space in between them to parallel the distance between the bilateral STNs. We lowered the electrodes bilaterally into the holes with the tips implanted at 8 mm depth below the cortical surface, according to the rat brain atlas (Paxinos and Watson, 1996). The electrodes' base, the plastic plate, and the screws were finally covered with dental cement. After suturing, wounds were treated with an analgesic (Ketofen, Centravet, France), Fucidin cream (Fucidine 2%, Laboratoires Leo, France) and iodine solution (Betadine Dermique 10%, Meda Pharma, France). All rats followed a post-operative antibiotic treatment (Duphamox, Fort Dodge, France). One week after implantation of the electrodes, a period of time during which the animals recovered from surgery, the stimulator container was connected to the electrode container and screwed on the plastic plate of the electrode container (Figure 2). This was done in the same conditions for the 6-OHDA-lesioned rats and Sham-operated rats.

2.3.1. Stimulation Hardware

The stimulator was designed to satisfy requirements linked with the experimental context. In order to ensure ease of movement, the stimulator containing the appropriate batteries were placed above the electrode container as illustrated in Figure 2.

The stimulator is based on a typical H-bridge structure to control the current injected to the electrode associated in the series with a blocking capacitor to ensure charge balancing, therefore maximizing the tissue safety. As illustrated on the top left of Figure 3, four electrically controlled switches are used to control the current and enable both cathodic (Φc) and anodic (Φa) stimulation phases. The H-bridge structure is directly connected to a voltage-supply-independent-controlled-current-source, which delivers a fixed value current whatever

the state of charge of the power source of the stimulator. The global structure is supplied by a DC/DC converter to reach the required voltage range compared to the current requirement. In our case, this voltage was fixed at around 17.4V after accurate characterization of the stimulation load impedance as previously reported (Kolbl et al., 2013). The switches, the current source, and the DC/DC converter are directly driven by a micro-controller (*Freescale MC9S08SH8*) that generates the correct current and time value received from a software interface described below.

The entire embedded system is battery powered. In order to limit the volume and weight of the stimulator, we first performed power optimization of the structure, especially on the embedded micro-controller without affecting the accuracy of the applied pulse durations; the time resolution was kept under 0.5µs to meet the charge balancing conditions. Then, a weight-limited battery (zinc/air) technology was chosen to enable a minimum of 7 consecutive days of simulation with the maximal current, pulse durations and frequency. Further details on the development and design strategy used have been previously described (Kolbl et al., 2016).

This circuit was realized with discrete components to achieve a low-cost stimulator suitable for a large scale of experiments. The final printed board contained all components, except the electrodes, and the blocking capacitor was fabricated on a 3x14mm large 6 layers 0.8mm Printed Circuit Board (PCB) technology. The circuit, batteries and electrodes were fixed on the skull using custom plastic packaging divided in two parts as illustrated in Figure 2:

- The electrode container, housing the electrodes, the blocking capacitor, and a connector were fixed during the implantation surgery. The electrodes were fabricated as coaxial structures from a platinum/iridium wire (Phymep, France) for the active pole and a stainless steel tube (Phymep, France) for the current return pole; the active pole is 1mm longer than the

current return pole in which the platinum/iridium wire is insulated. Both electrodes in the right and left hemispheres were connected in parallel for approximately equal current repartition as the right and left electrodes have the same geometry and thus the same impedance.

- The stimulator container includes three zinc/air batteries (*Power One p675 Implant Plus*) and the PCB board. The top of the box includes a drilled column for the system to be screwed to the electrode container and turn on the global system by contacting both poles of the electrical supply. This particularity enabled battery changes without additional surgery and the continuation of experiments lasting longer than one week. All mechanical parts were fabricated with natural polylactic acid polymer.

2.3.2. Stimulus tuning and software control

The stimulator is programmed with the animal awake and free of movement. Only a cable is connected to the stimulator container during observation for stimulus tuning. The pressure on the connector is light to avoid the risk to hurt the animal in case of sudden movement. The stimulus programming cable is connected from the RS232 interface of the stimulator to a computer through a FTDI RS232 to USB converter as shown in Figure 4.

A dedicated software interface has been developed as shown in the right part of Figure 4, permitting half duplex communication with the stimulator. At the connection initialization, the stimulator systematically sends a unique identification number to save and store waveform parameters for each animal of a population, and a flag appears if stimulation is currently ON. The stimulation can be turned ON and OFF by the software, and a large set of parameters can be loaded only when the stimulation is OFF. As summarized in Table 1, the stimulator has been designed to deliver a wide range of frequencies, pulse widths, cathodic and anodic current amplitudes, and cathodic and inter-pulse durations. All these parameters can be

chosen in the ranges presented in Table 1 and are defined by the user, except for the charge balancing which is automatically processed by the software through the anodic duration computation. A secondary panel can be opened for accurate observation of the stimulation threshold by increasing the stimulation amplitude with a current fixed step. This option permits fast and easy waveform tuning on the freely moving animal without focusing on the entire set of parameters. For example, the applied parameters can be saved and loaded again after battery changes on both interfaces.

2.3.3. Stimulation parameters

As the present work has been done in the context of PD, the parameters chosen for chronic stimulation in rats were similar to those used in DBS parkinsonian patients with a frequency of 130 Hz, pulse width of 0.06 ms (Limousin et al., 1998; Krack et al., 2003). The current intensities were determined for each rat below the values inducing motor side effects, and the average stimulus intensity used was about 300 µA.

2.4. *In vivo* validation of the stimulator

Behavioural experiments began after the pacemaker was connected to the electrodes and placed on the animals' heads. After finishing the behavioural tests in the control situation (stimulation OFF), the stimulation was turned ON and maintained continuously for one week. Then, the rats were submitted to the behavioural tests.

2.4.1. Evaluation of locomotor activity

Rat spontaneous locomotor activity was assessed using an Open Field Actimeter (Imetronic, France) as previously described (Delaville et al., 2012; Bouabid et al., 2014). The actimeter consisted of a transparent platform (60x60 cm) equipped with photoelectric cells. Light beams detected movement, and the total locomotor activity of each rat was recorded in two

consecutive sessions of 10 minutes. All tests in the actimeter were done on the fourth day, after 3 days of habituation, in an isolated room between 8:00 a.m. and 1:00 p.m. The parameters analysed included the number of both horizontal and vertical movements and the distance travelled by the animals.

2.4.2. Assessment of motor coordination

The effect of 6-OHDA lesions and STN HFS on motor coordination was investigated through training the rats to remain on a rotarod (Bioseb, in vivo Research Instruments, Spain), as previously described (Bouabid et al., 2014). During the training period of 3 days, each rat was placed on a horizontal rod (7 cm diameter) rotating at a gradually increasing speed from 4 to 20 rotations per minute (rpm) for a maximum of 15 min, by which time a steady baseline level of performance was reached. During the fourth day, the motor coordination was recorded for each animal over three trials. The latency to fall off the rotarod was recorded and the time limit was fixed at 3 minutes. The mean time of the three trials was used for analysis.

2.5. Histology and immunohistochemistry

Histology and immunohistochemistry were performed to validate the position of the stimulating electrodes in the STNs and the extent of dopamine cell denervation respectively.

After completion of the experiments, rats were deeply anaesthetized and perfused transcardially with saline (0.9%) followed by a fixative 4% paraformaldehyde in 0.1 M PBS (pH: 7.4). The brains were removed, post-fixed 4 hours in the same fixative, and placed in 0.1 M PBS with 20% sucrose overnight. The brains were frozen in isopentane at –40°C and stored at –80°C. They were then cut into 50 µm coronal sections using a cryotome, and slices were stored in 0.1 M PBS containing 0.2% sodium azide. Cresyl violet staining of slices containing the STN was used to determine the location of the stimulating electrodes as

previously described (Tai et al., 2003). To determine the extent of lesion of the nigro-striatal dopaminergic pathways, we used immunohistochemical staining of tyrosine hydroxylase (TH) as previously described (Bouali-Benazzouz et al., 2009; Faggiani et al., 2018).

2.6. Statistical analysis

Statistical analyses were done using Sigma Plot program (Systat Software, San Jose, USA). Behavioral data from 6-OHDA and sham animals were compared using Mann Whitney tests. Then, the parameters of behavioral tests in 6-OHDA lesioned rats with and without STN-HFS were compared using Wilcoxon t-tests.

3. Results

In accordance with animal ethics, we have limited the number of rats used in the study. A total of 24 rats were used to test our new device. The animals were observed and handled daily throughout all the experimentation. The stimulation device was well tolerated and the animals maintained a good general welfare without any visible discomfort. Their hair has not been bristled and the animals have not lost weight. As the mechanical parts were fabricated with natural polylactic acid polymer, there were no skin inflammatory reactions, infections or rejection phenomena against the containers. At the end, 12 rats with a precise bilateral implantation of stimulation electrodes in the NST (six sham-operated rats and six 6-OHDA-lesioned rats) with a total or subtotal bilateral lesion of the dopaminergic neurons of the SNc (the six 6-OHDA rats) were retained for the analysis of their data (see section 3.3. histological and immunohistochemical controls).

3.1. Effects of 6-OHDA lesion and STN-HFS on locomotor activity

As expected, and compared to sham-operated rats, bilateral 6-OHDA injections affected locomotor activity by significantly decreasing the number of spontaneous horizontal

movements from 2063.20±322.90 to 1135.50±168.00 (Mann-Whitney test, p=0.002, Fig. 5A), the number of vertical movements from 55.00±7.00 to 27.30±4.90 (Mann-Whitney test, p=0.002, Fig. 5B), and the distance traveled in the open-field from 270.50±33.50 to 137.50±33.80 m (Mann-Whitney test, p=0.002, Fig. 5C). On the other hand, STN-HFS improved the locomotor deficit induced by 6-OHDA as it significantly increased the number of horizontal movements to 1838.00±183.70 (Wilcoxon test, p=0.031 Fig 5A), the number of vertical movements to 49.50±8.70 (Wilcoxon test, p=0.031 Fig. 5B), and the distance traveled by the animals to 250.20±36.50 m (Wilcoxon test, p=0.031 Fig. 5C), when compared to the values obtained in the same 6-OHDA lesioned animals without STN-HFS. The values obtained with STN-HFS were not significantly different from those obtained in sham-operated animals (Mann-Whitney test, p=0.309 Fig. 5A, p=0.394 Fig. 5B, p=0.623 Fig. 5C, respectively).

3.2. Effects of 6-OHDA lesion and STN-HFS on motor coordination

In addition to the spontaneous locomotor activity, we determined whether STN-HFS could improve motor coordination deficits induced by 6-OHDA using the rotarod test. Only animals with good performance during the training period of 3 days were included in the study. From the twelve rats, five 6-OHDA-lesioned and four sham-operated animals were selected for statistical analysis of data. Our results showed that 6-OHDA lesions significantly reduced the time spent on the rotarod bar when compared to sham operated animals (283.50±16.50 sec vs 181.60±21.04 sec, Mann-Whitney test, p=0,0049, Fig. 6). STN-HFS restored motor coordination by significantly increasing the time spent on the rotarod bar compared to the values obtained in the same 6-OHDA lesioned animals without STN-HFS (256.00±35.20 sec, Wilcoxon matched-pairs test, p=0.046, Fig 6). The values obtained with STN-HFS in sham-operated animals were not significantly different (Mann-Whitney test, p=0.349, Fig. 6).

3.3. Histological and immunohistochemical controls

All the selected animals, which received a bilateral 6-OHDA injection into the MFB showed a subtotal or total loss of TH-immunoreactive cell bodies in the SNc and fibers in the striatum when compared to sham operated animals (Fig. 7A-D). Additionally, all the animals selected for the analysis of data showed a correct bilateral placement of the electrodes within the STN (Fig. 7E-F).

4. Discussion

Most of the studies with electrical stimulation in freely moving rodents use a rotating wire placed over the animals' cage (Salin et al., 2002; Baunez et al., 2007; Temel et al., 2005; Pelloux et al., 2018; van Zwieten et al., 2019). This limited the duration and number of behavioral tests as the animal had a wire plugged over the skull. To improve these limitations, several embedded DBS systems have been designed for rodents. A comparison of the existing embedded stimulators for rodents is summarized in Table 2.

In this present study, we successfully developed and validated a new implantable stimulator for freely moving rats that can be used for different deep brain structures in animal models of brain diseases. One of the major advantages of the present stimulator is the choice to use bilateral or unilateral stimulation. Here, we validated the device by using bilateral STN stimulation, as the tests were done on a bilateral 6-OHDA rat model to mimic the advanced stage of PD. For bilateral stimulation, only one stimulation channel was needed, and the delivered current had to be divided by 2 to calculate the exact current intensity injected in each hemisphere. To our knowledge, compared to the existing wireless stimulators reported in the literature (see also Ewing and Grace, 2013), this is the first device that combines the ability to stimulate bilaterally or unilaterally with other important functions (described below

and in Table 2) that reproduce the pacemaker characteristics used in patients, and meets all the safety conditions.

Another important characteristic of the stimulator includes the biphasic current-control and charge balancing, which allows for maximized tissue safety, in contrast to the monopolar square stimulations which causes a high risk of lesions (Meissner et al., 2004). In this study, it has been shown that a monopolar monophasic charge-balanced current induced extensive brain tissue damage in a non-human primate study. The circuit that we developed in the present device is in charge of delivering the adequate current to the tissue and may work under a high output voltage considering the impedance loading with respect to charge balancing. In addition, the device proposes large ranges of the stimulation parameters, including the frequency, pulse width. and current intensities. We used STN-HFS in the context of PD, nevertheless, it can be very important and mandatory to use low frequency stimulations for other neurological and psychiatric pathologies. For example, the majority of studies using pedunculopontine nucleus stimulation for PD gait freezing reported that its efficacy was obtained at frequencies lower than 60-80 Hz with a maximal effect at 20-35 Hz (*for review*, Thevathasan et al., 2018).

The batteries have a minimum life duration of 7 days when the stimulator is ON at the highest level of intensity. For chronic stimulation tests with longer duration of the experiments, the batteries can be quickly and easily changed. It is possible to simply unscrew the screw, remove the pacemaker cover, and remove the batteries to replace them with new ones.

Notably, the stimulator container, with all the electronic parts, is totally independent of the electrode container and is removable and reusable. The front-end stimulation is the only part of the DBS device directly connected to the electrodes. Moreover, the implementation of the stimulator relies on a programmable microcontroller. This choice enables future changes in

the stimulation waveform and stimulation strategy to adapt to different pathological contexts and to test new stimulation methods. A detailed description of the circuit design, architecture, and sizing, as well as considerations on power optimization, battery selection, and the specificities of the package attached to the implanted electrodes have been reported previously (Kölbl et al., 2016).

Instead of implanting the stimulator in the abdomen or in a jacket, we preferred to attach the stimulator on the electrode container without any contact with the animals' skin to avoid the risk of inflammation and infection. Several studies developed a stimulator implanted in the abdominal area of rodents that connects to an electrode implanted into the brain (Russold and Jarvis, 2007; Harnack et al., 2008). This system, which requires biocompatible materials, not only presents a risk of infection but additionally limits the programming of the stimulation parameters, as the animal must be placed in a tubular device. In this condition, the movements are restricted, and the behavioral effects of DBS cannot be evaluated during programming (Harnack et al., 2008). Another limitation is that the battery is implanted with the circuit inside the animal body, thus requiring additional surgery to be changed and resulting in additional risk of infection. Another wearable stimulator placed in a vest has been described by two teams (Lee et al., 2010; Nowak et al., 2011). Although both systems meet the electrical requirements of brain tissue safety, the experiments are limited by tearing of the vest and the risk of brain damage if the electrodes are pulled out, as well as the infectious risk at the level of the exit of the cable connection to the pacemaker located in the vest.

To maximize safety conditions, we additionally added a reset button that allows the experimenter to stop the stimulation in case of emergency. The programmed parameters will not be erased but can be controlled and modified by connecting the stimulator to the interface and switching it ON again.

Finally, our system has been validated in the bilateral 6-OHDA rat model, which is characterized by severe motor deficits mimicking the advanced stages of PD. As predicted and similarly to patients with advanced stage PD, STN stimulation at high frequency dramatically improved locomotor activity and motor coordination. This demonstrates that the stimulation parameters and the programmed settings used were able to restore the motor deficits induced by the bilateral dopamine depletion in bilateral 6-OHDA rats. In general, during chronic stimulation, all the implanted animals maintained an overall good general welfare without discomfort. The device was well tolerated by all the animals used in this study, and there were no observations of skin inflammatory reactions nor infection or rejection phenomena.

In conclusion, we successfully developed and validated a new implantable stimulator for freely moving rats, respecting a maximum similarity with the pacemaker used in patients. It is characterized by bilateral stimulation, biphasic current-control, and charge balancing to maximize the tissue safety and wide range of frequencies, pulse widths, and current intensities. The device is also characterized by its adapted stimulation waveforms, stimulation circuitry for low power consumption, and high capacity batteries. Furthermore, dedicated software has been developed to program the stimulation parameters, including the frequency, pulse width, and current intensity. The present stimulator can be used in different animal models of brain diseases for different deep brain structures.

Acknowledgements: This work was supported by the Labex Brain (PD-PAIN 2017-0410), Centre National de la Recherche Scientifique and Université de Bordeaux. We wish to thank Miss Sara Whitestone for proof reading of the manuscript.

References

Baunez, C., Christakou, A., Chudasama, Y., Forni, C. and Robbins, T.W., 2007. Bilateral high-frequency stimulation of the subthalamic nucleus on attentional performance: transient deleterious effects and enhanced motivation in both intact and parkinsonian rats. Eur J Neurosci. 25, 1187-1194.

Benazzouz, A., Gross, C., Feger, J., Boraud, T., Bioulac, B., 1993. Reversal of rigidity and improvement in motor performance by subthalamic high-frequency stimulation in MPTP-treated monkeys. Eur. J. neurosci. 5**,** 382-389.

Benazzouz A1, Hallett M., 2000. Mechanism of action of deep brain stimulation. Neurology 55(12 Suppl 6), S13-16.

Bouabid S, Delaville C, De Deurwaerdère P, Lakhdar-Ghazal N, Benazzouz A., 2014. Manganese-induced atypical parkinsonism is associated with altered Basal Ganglia activity and changes in tissue levels of monoamines in the rat. PLoS One. 9(6):e98952. doi: 10.1371/journal.pone.0098952.

Bouali-Benazzouz, R., Tai, C.H., Chetrit, J. and Benazzouz, A., 2009. Intrapallidal injection of 6-hydroxydopamine induced changes in dopamine innervation and neuronal activity of globus pallidus. Neuroscience. 164, 588-596. doi: 10.1016/j.neuroscience.2009.07.034.

Delaville, C., Chetrit, J., Abdallah, K., Morin, S., Cardoit, L., De Deurwaerdere, P., Benazzouz, A., 2012. Emerging dysfunctions consequent to combined monoaminergic depletions in Parkinsonism. Neurobiol Dis 45, 763-773. doi: 10.1016/j.neuroscience.2011.11.024.

Ewing, S.G. and Grace, A.A., 2013. Long-term high frequency deep brain stimulation of the nucleus accumbens drives time-dependent changes in functional connectivity in the rodent limbic system. Brain Stimul., 6, 274-85. doi: 10.1016/j.brs.2012.07.007.

Faggiani E. and Benazzouz A., 2017. Deep brain stimulation of the subthalamic nucleus in Parkinson's disease: From history to the interaction with the monoaminergic systems. Prog Neurobiol. 151, 139-156. doi: 10.1016/j.pneurobio.2016.07.003.

Faggiani, E., Delaville, C., Benazzouz, A., 2015. The combined depletion of monoamines alters the effectiveness of subthalamic deep brain stimulation. Neurobiol. Dis., 82, 342-348. doi: 10.1016/j.nbd.2015.07.010.

Faggiani E, Naudet F, Janssen MLF, Temel Y, Benazzouz A., 2018. Serotonergic neurons mediate the anxiolytic effect of l-DOPA: Neuronal correlates in the amygdala. Neurobiol. Dis., 110, 20-28. doi: 10.1016/j.nbd.2017.11.001.

Fluri, F., Mützel, T., Schuhmann, M.K., Krstić, M., Endres, H. and Volkmann J., 2017. Development of a head-mounted wireless microstimulator for deep brain stimulation in rats. J Neurosci Methods., 291, 249-256. doi: 10.1016/j.jneumeth.2017.08.024.

Forni, C., Mainard, O., Melon, C., Goguenheim, D., Kerkerian-Le Goff, L., and Salin, P., 2012. Portable microstimulator for chronic deep brain stimulation in freely moving rats. J. Neurosci. Methods 209, 50–57. doi: 10.1016/j.jneumeth.2012.05.027

Kölbl, F., Sabatier, J., N'Kaoua, G., Naudet, F., Faggiani, E., Benazzouz, A., Renaud, S. and Lewis, N., 2013. Characterization of a non linear fractional model of electrode-tissue impedance for neuronal stimulation. In Biomedical Circuits and Systems Conference (BioCAS), 2013 IEEE, pp. 338-341.

Kölbl, F., N'Kaoua, G., Naudet, F., Berthier, F., Faggiani, E., Renaud, S., Benazzouz, A. and Lewis, N., 2016. An Embedded Deep Brain Stimulator for Biphasic Chronic Experiments in Freely Moving Rodents. IEEE Trans Biomed Circuits Syst. 10:72-84. doi: 10.1109/TBCAS.2014.2368788.

Harnack, D., Meissner, W., Paulat, R., Hilgenfeld, H., Müller, W.D., Winter, C., Morgenstern, R. and Kupsch, A., 2008. Continuous high-frequency stimulation in freely moving rats: development of an implantable microstimulation system. J. Neurosci. Methods. 167, 278-291.

Hentall, I.D., 2013.A long-lasting wireless stimulator for small mammals. Front Neuroeng. 6, 8. doi: 10.3389/fneng.2013.00008.

Krack, P., Batir, A., Van Blercom, N., Chabardes, S., Fraix, V., Ardouin, C., Koudsie, A., Limousin, P.D., Benazzouz, A., LeBas, J.F., Benabid, A.L., Pollak, P., 2003. Five-year follow-up of bilateral stimulation of the subthalamic nucleus in advanced Parkinson's disease. N. Engl. J. Med. 349, 1925-1934.

Krack, P., Hariz, M.I., Baunez, C., Guridi, J., Obeso, J.A., 2010. Deep brain stimulation: from neurology to psychiatry? Trends Neurosci. 33, 474-484. doi.org/10.1016/j.tins.2010.07.002.

Lang AE, Lozano AM., 1998. Parkinson's disease. Second of two parts. N. Engl. J. Med. 339, 1130-1143.

Lee, J., Rhew, H.G., Kipke, D.R. and Flynn, M.P., 2010. A 64 channel programmable closed-loop neurostimulator with 8 channel neural amplifier and logarithmic ADC," IEEE J. Solid-State Circuits, vol. 45, no. 9, pp. 1935–1945.

Limousin, P., Pollak, P., Benazzouz, A., Hoffmann, D., Le Bas, J.F., Broussolle, E., Perret, J.E., Benabid, A.L., 1995. Effect of parkinsonian signs and symptoms of bilateral subthalamic nucleus stimulation. Lancet 345, 91-95.

Limousin, P., Krack, P., Pollak, P., Benazzouz, A., Ardouin, C., Hoffmann, D., Benabid, A.L., 1998. Electrical stimulation of the subthalamic nucleus in advanced Parkinson's disease. N. Engl. J. Med. 339:1105-1111.

Liu, X., Demosthenous, A. and Donaldson, N., 2010. A dual-mode neural stimulator capable of delivering constant current in current-mode and high stimulus charge in semi-voltage-mode. In Proc. IEEE Int. Symp. Circuits and Systems, May 2010, pp. 2075–2078.

Meissner W, Gross CE, Harnack D, Bioulac B, Benazzouz A. 2004. Deep brain stimulation for Parkinson's disease: Potential risk of tissue damage associated with external stimulation. Ann Neurol., 55, 449-50.

Meissner, W., Leblois, A., Hansel, D., Bioulac, B., Gross, C.E., Benazzouz, A., Boraud, T., 2005. Subthalamic high frequency stimulation resets subthalamic firing and reduces abnormal oscillations. Brain, 128, 2372-2382.

Nowak, K., Mix, E., Gimsa, J., Strauss, U., Sriperumbudur, K.K., Benecke, R. and Gimsa, U., 2011. Optimizing a rodent model of Parkinson's disease for exploring the effects and mechanisms of deep brain stimulation. Parkinsons. Dis., 2011, 414682. doi: 10.4061/2011/414682.

Paxinos, G. and Watson, C., 1996. The Rat Brain in Stereotatic Coordinates. Academic Press, San Diego.

Pelloux, Y., Degoulet, M., Tiran-Cappello, A., Cohen, C., Lardeux, S., George, O., Koob, G.F., Ahmed, S.H. and Baunez, C., 2018. Subthalamic nucleus high frequency stimulation prevents and reverses escalated cocaine use. Mol Psychiatry. 23, 2266-2276. doi: 10.1038/s41380-018-0080-y.

Russold, M. and Jarvis, J.C., 2007. Implantable stimulator featuring multiple programs, adjustable stimulation amplitude and bi-directional communication for implantation in mice. Med. Biol. Eng. Comput., 45, 695-699.

Salin, P., Manrique, C., Forni, C., Kerkerian-Le Goff, L., 2002. High-frequency stimulation of the subthalamic nucleus selectively reverses dopamine denervation-induced cellular defects in the output structures of the basal ganglia in the rat. J. Neurosci. 22, 5137-5148.

Schor, J.S. and Nelson, A.B., 2019. Multiple stimulation parameters influence efficacy of deep brain stimulation in parkinsonian mice. J Clin Invest. 2019 Jun 13;130:3833-3838. doi: 10.1172/JCI122390.

Tai, C.H., Boraud, T., Bezard, E., Bioulac, B., Gross, C., Benazzouz, A., 2003. Electrophysiological and metabolic evidence that high-frequency stimulation of the subthalamic nucleus bridles neuronal activity in the subthalamic nucleus and the substantia nigra reticulata. FASEB journal 17, 1820-1830.

Temel, Y., Visser-Vandewalle, V., Aendekerk, B., Rutten, B., Tan, S., Scholtissen, B., Schmitz, C., Blokland, A., Steinbusch, H.W., 2005. Acute and separate modulation of motor and cognitive performance in parkinsonian rats by bilateral stimulation of the subthalamic nucleus. Exp. neurol. 193, 43-52.

Thevathasan, W. and Moro, E., 2019. What is the therapeutic mechanism of pedunculopontine nucleus stimulation in Parkinson's disease? Neurobiol. Dis., 128, 67-74. doi: 10.1016/j.nbd.2018.06.014.

van Zwieten, G., Jahanshahi, A., van Erp, M.L., Temel, Y., Stokroos, R.J., Janssen, M.L.F. and Smit, J.V., 2019. Alleviation of Tinnitus With High-Frequency Stimulation of the Dorsal

Cochlear Nucleus: A Rodent Study. Trends Hear. 23, 2331216519835080. doi: 10.1177/2331216519835080.

Figure legends

Figure 1. Schematic presentation of the experimental paradigm.

Figure 2. Schematic representation of the stimulator and the implantation procedure. The electrode container is the only part fixed during surgery. The stimulator container is fixed to the electrode container by a central screw. It contains both circuits and changeable Air/zinc batteries.

Figure 3. Circuit diagram of the stimulation device. The pacemaker circuit is embedded on the rodent in the stimulator container and composed of three mains parts: first the current source with the H bridge, delivering cathodic and anodic current pulses, second the DC/DC converter generating the high-level voltage (17,6V) imposed by electrode impedance, and thirds the microcontroller generating the correct stimulation waveform. Waveform programing is performed by a software by UART/USB FTDI converter.

Figure 4. Overview of the software interface during the experimentations. A main panel permits to control all parameters of the wave shape (frequency, current levels and timings) except the anodic timing, which is automatically computed respecting charge balancing. A secondary panel enables incrementation/decrementation of current levels with reduced operation to focus on animal behaviour.

Figure 5: Effect of 6-OHDA lesion of the nigro-striatal pathway and STN-HFS on locomotor activity recorded in the open field actimeter. Histograms showing the number of spontaneous horizontal movements (A) the number of vertical movements (B) and the distance traveled by the animals (C) in sham-operated rats (Sham, n=6) and 6-OHDA-lesioned rats (n=6) without

(6-OHDA Stim OFF) and with STN-HFS (6-OHDA Stim ON). Values are the mean ± SEM. **: $p<0.01$ in comparison with sham-operated animals; #: $p<0.05$ in comparison with 6-OHDA-lesioned rats without STN-HFS.

Figure 6: Effect of 6-OHDA lesion of the nigro-striatal pathway and STN-HFS on movement coordination. Histograms showing the time spent by the animals on the rotating bar of the rotarod in sham-operated rats (Sham, n=4) and 6-OHDA-lesioned rats (n=5) without (6-OHDA Stim OFF) and with STN-HFS (6-OHDA Stim ON). Values are the mean ± SEM. **: $p<0.01$ in comparison with sham-operated animals; #: $p<0.05$ in comparison with 6-OHDA-lesioned rats without STN-HFS.

Figure 7: Representative examples of brain slices showing TH immunoreactive neurons in the pars compacta of substantia nigra (A-B) and fibers in the striatum (C-D) of sham-operated rats (left, n=6) and 6-OHDA-lesioned rats (right, n=6). E: A coronal diagram from the rat brain atlas of Paxinos and Watson (1996) showing the stereotaxic location of the STN in the two hemispheres. F: A representative example of a rat brain slice showing the location of the stimulating electrodes implanted bilaterally with the tips in the STN.

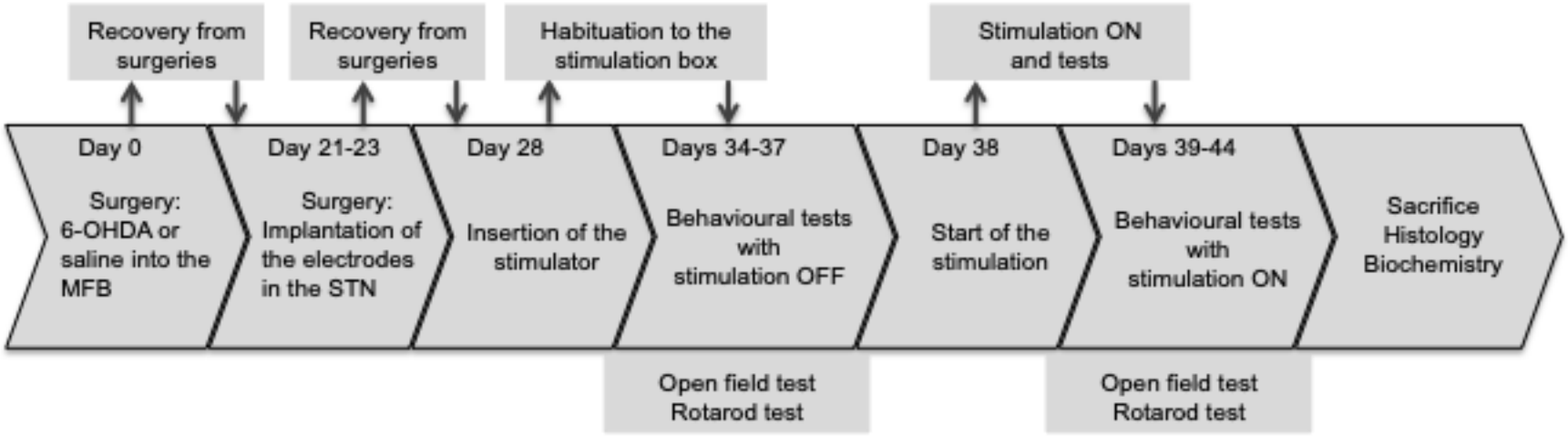
Recovery from surgeries
Recovery from surgeries
Habituation to the stimulation box
Stimulation ON and tests
Day 0
Surgery: 6-OHDA or saline into the MFB
Day 21-23
Surgery: Implantation of the electrodes in the STN
Day 28
Insertion of the stimulator
Days 34-37
Behavioural tests with stimulation OFF
Day 38
Start of the stimulation
Days 39-44
Behavioural tests with stimulation ON
Sacrifice
Histology
Biochemistry
Open field test
Rotarod test
Open field test
Rotarod test

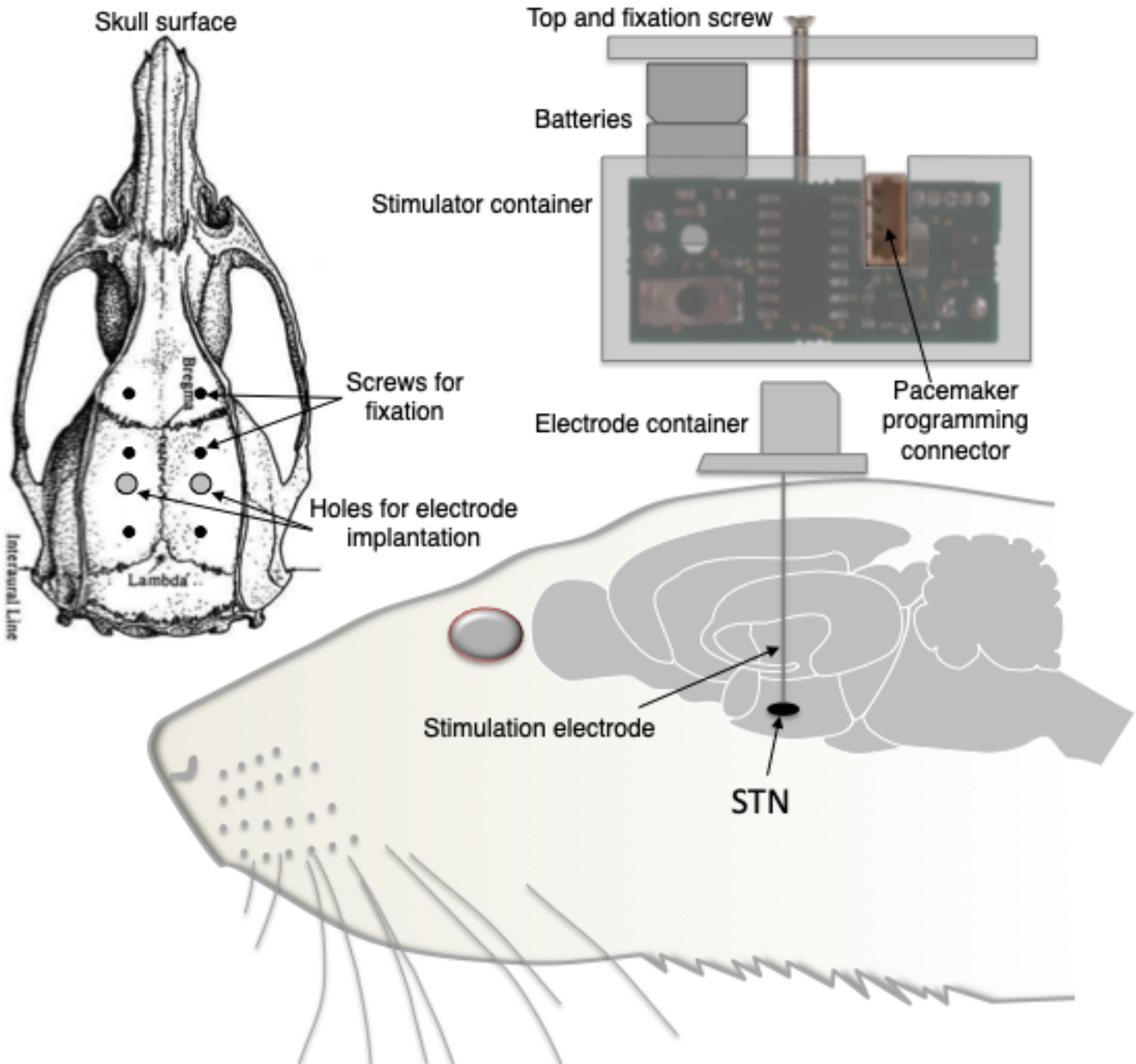
Skull surface
Top and fixation screw
Batteries
Stimulator container
Screws for fixation
Pacemaker programming connector
Electrode container
Holes for electrode implantation
Bregma
Lambda
Interaural Line
Stimulation electrode
STN

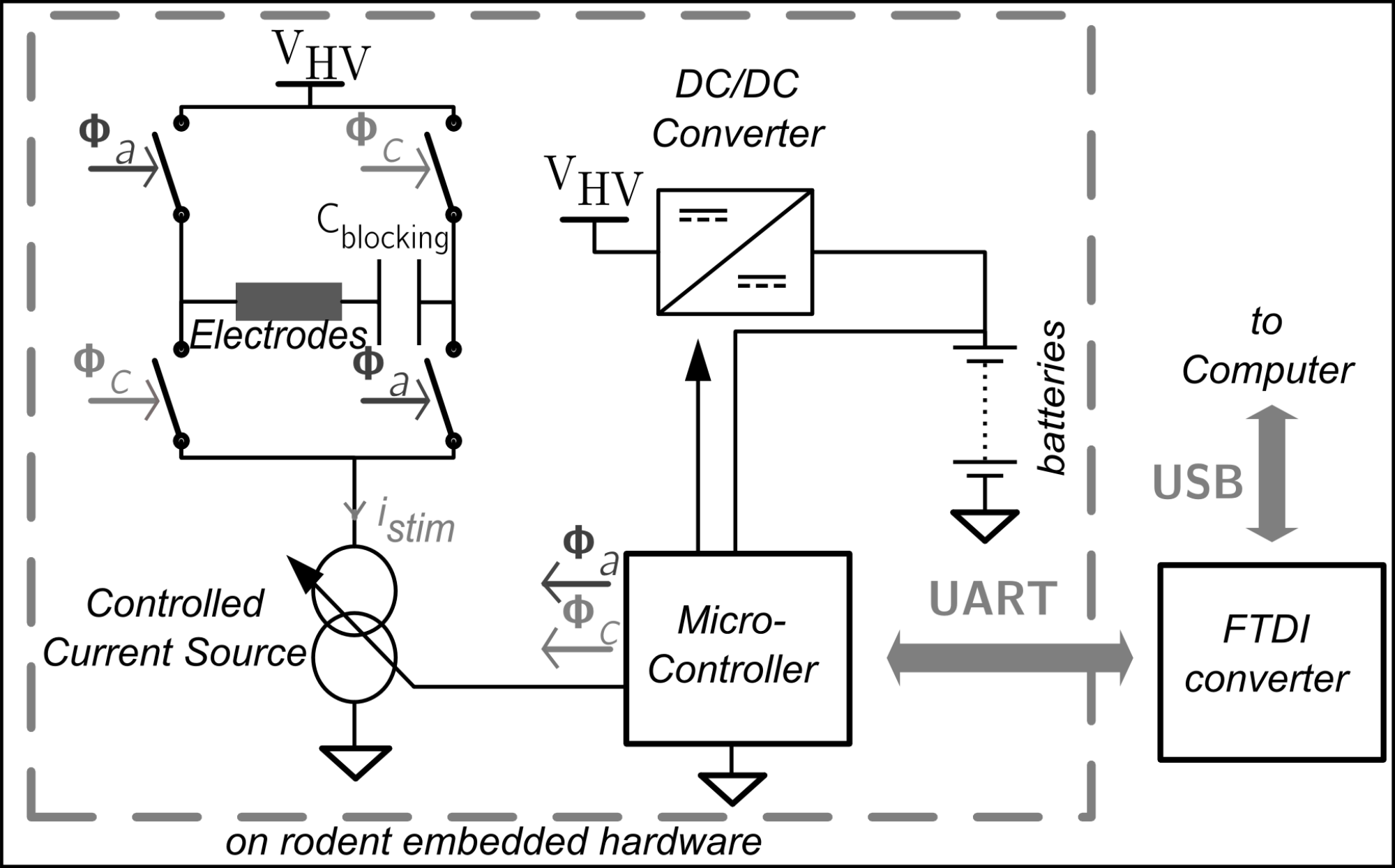
V_{HV}
Φ_a
Φ_c
$C_{blocking}$
Electrodes
Φ_c
Φ_a
i_{stim}
Controlled
Current Source
DC/DC
Converter
V_{HV}
batteries
Φ_a
Φ_c
Micro-
Controller
UART
to
Computer
USB
FTDI
converter
on rodent embedded hardware

Awake freely moving rat

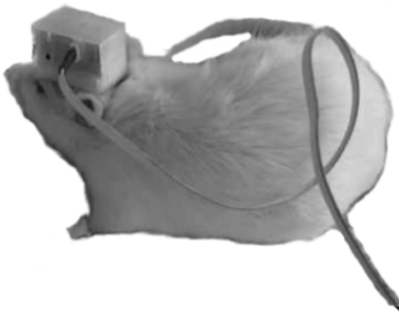

Computer (software main window)

USB connection
(programming of
stimulation parameters)

Secondary control panel
(adjustment of parameters
by observing rat behaviour)

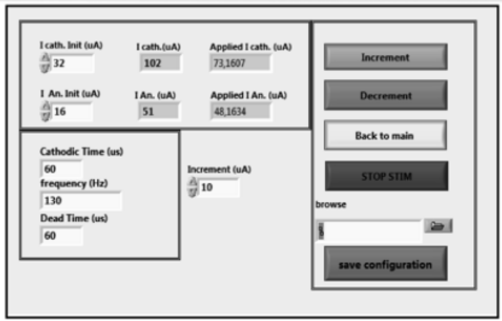

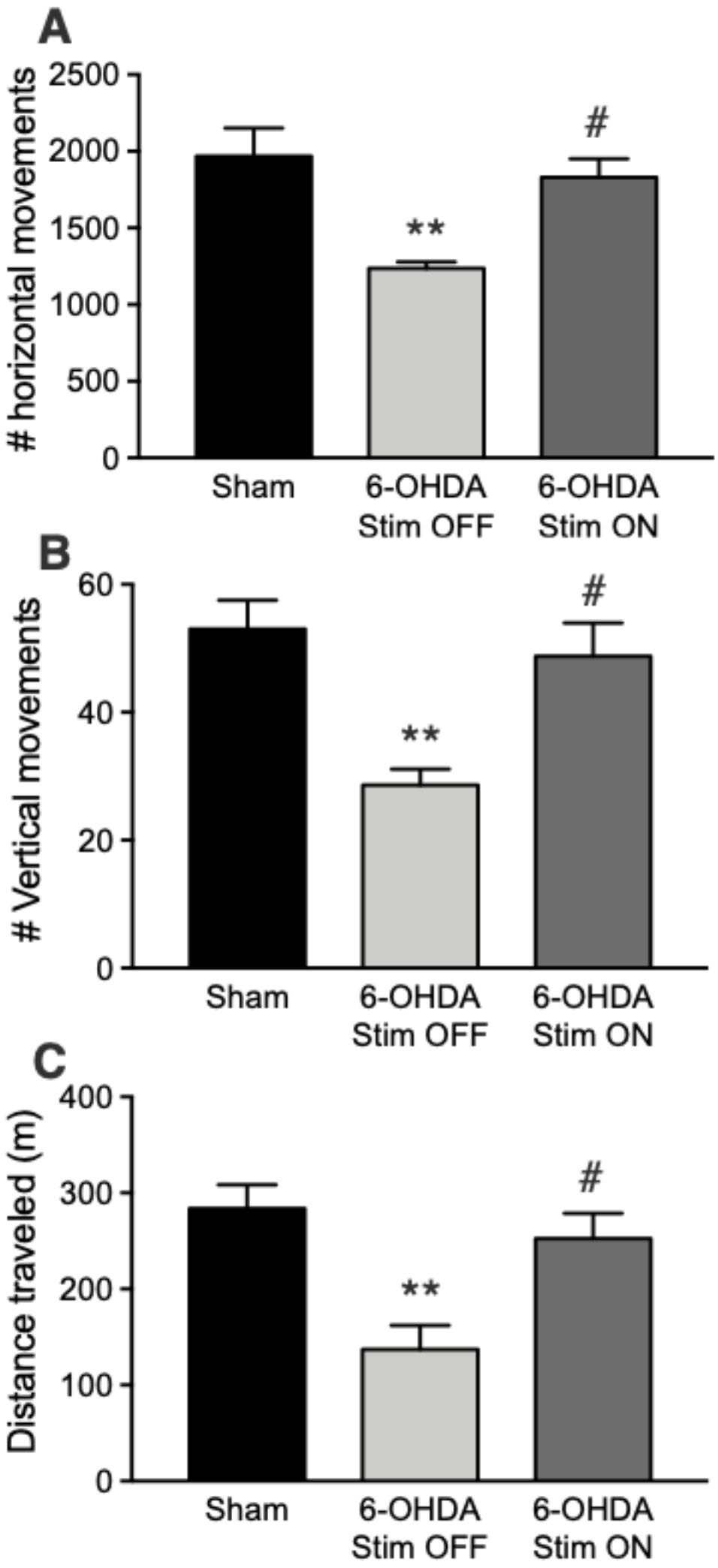
A
horizontal movements
2500
2000
1500
1000
500
0
**
#
Sham
6-OHDA Stim OFF
6-OHDA Stim ON
B
Vertical movements
60
40
20
0
**
#
Sham
6-OHDA Stim OFF
6-OHDA Stim ON
C
Distance traveled (m)
400
300
200
100
0
**
#
Sham
6-OHDA Stim OFF
6-OHDA Stim ON

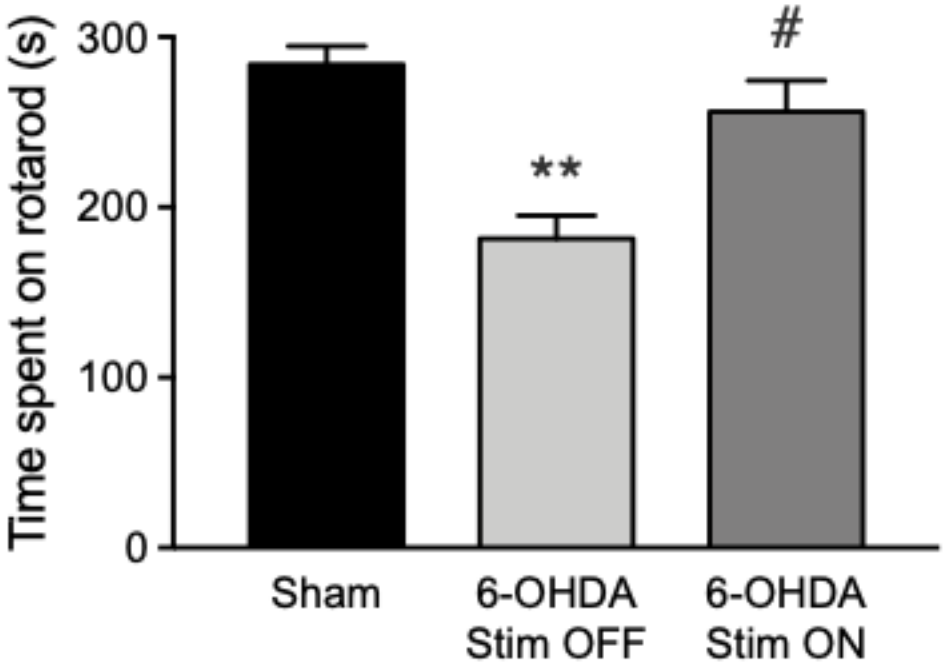
Time spent on rotarod (s)
300
200
100
0
**
#
Sham
6-OHDA
Stim OFF
6-OHDA
Stim ON

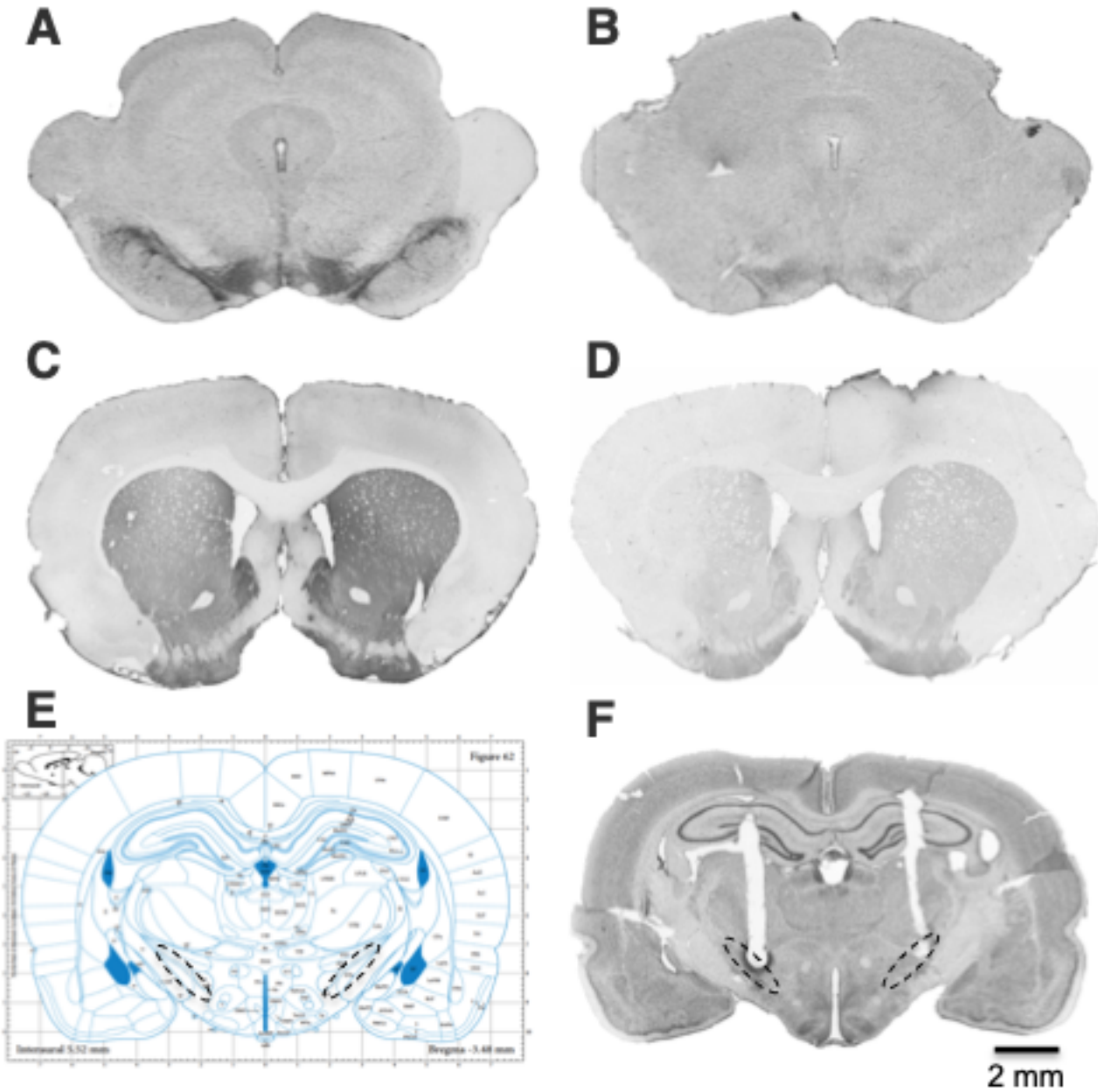
A
B
C
D
E
F
2 mm

Table 1 : Summary of electrical micro-stimulation system performances as measured during in vitro experiments.

Characteristics	**Measured value**	**Accuracy**
Weight	13.8g	
Size (W/L/H)	22.2/32.8/23mm	
Power Supply	4.8V (open circuit, in charge: 3.6V)/675 mAh	
Maximal electrode voltage	17V	
Batteries life time	> 7 days	
Range of current intensity	20 µA - 2000 µA (10 µA – 1000 µA/hemisphere)	relative deviation < 1%
Range of frequency	1 - 300Hz	< ±0.01Hz
Pulse width	40 - 1000 µs	±0.25µs

Table 2: Comparison of the existing stimulators

References	Bilateral stimulation	Stimulation mode (I or V)	Range of stimulation	Biphasic stimulation	Nature of implantation	Programmable	changes in the stimulation waveform	Removable system	Battery Accessibility during experiment
Russold et al. 2007	No	V	0 - 3 V	No	Inside the body	Yes	-	No	No
Harnack et al. 2008	No	I	50 - 600 μA	Yes	Inside the body	Yes	-	No	No
Liu et al. 2008	No	I	200 - 500 μA	No	On the head	-	-	No	No
Lee et al. 2008	No	I	3 - 135 μA	No	In a jacket	Yes	-	Yes	Yes
Hentall et al., 2010	No	I	-	-	On the head	-	-	No	No
Nowak et al. 2011	No	-	-	Yes	In a jacket	No	-	Yes	Yes
Forni et al. 2012	No	I	50 - 120 μA	Portable on the head	On the head	No	-	Yes	Yes
Ewing et al. 2013	Yes	I	15 - 50 μA	No	On the head	Yes	-	No	No
Fluri et al. 2017	No	I	10 - 500 μA	Yes	On the head	Yes	-	Yes	Yes
The present study	Yes	I	20 - 2000 μA	Yes	On the head	Yes	Yes	Yes	Yes